

# THREE DIMENSIONAL METHOD FOR MONITORING DAMAGE TO DOLOS BREAKWATERS

Kishan Tulsi<sup>1</sup>, Koos Schoonees<sup>2</sup>, Magenthran Ruthenavelu<sup>3</sup>, Gregory Davids<sup>1</sup>,  
Robert Vonk<sup>1</sup>, Francios Stroh<sup>4</sup> and Nic Herrington<sup>5</sup>

In order to extend the design life of breakwaters, regular damage investigations and timeous repairs are required. One of the important aspects is calculating the severity of damage to breakwaters. Traditionally, breakwater inspection has been done using aerial photographs and underwater imaging to accomplish these investigations. Breakwaters are systematically divided into inspection stations and photographs are taken to inspect and assess the damage. The photographs are then visually compared with the previous inspection photographs to identify changes. This is difficult to achieve as it is not always possible to get the helicopter exactly in the same position on every survey and highly dependent on the skill of the helicopter pilot. Another difficulty is taking underwater images near the breakwater due to poor visibility and wave breaking. The objective of this study is to test a 3D analysis method by evaluating the accuracy of using the LIDAR and multi-beam echo sounder data to quantify damage to dolos breakwaters above and below the water surface (including the inter-tidal zone). Thus, this comparison is aimed towards the development of the 3D eroded volume method (3D method).

*Keywords: rubble-mound breakwater damage monitoring; LIDAR, multi-beam; turbulence modeling*

## INTRODUCTION

The present way of conducting dolos breakwater assessments in reality is the aerial photographic method. However, it is limited to the above water section and does not cover the underwater portion of the dolos slope. This has been compensated by quantifying the damage above water and multiplying it by a damage factor of 1.5 to accommodate the one third portion underwater but still within the active zone (Phelp and Zwamborn 2000). This is a major limitation of the photographic method and alternatives are needed to assess dolos breakwaters.

Recent advancements in technology have assisted in combining two survey instruments for use in monitoring of breakwaters. These are the laser scanner, which is primarily used for terrestrial surface mapping, and the multi-beam echo sounder used for mapping of bridges in navigation channels to identify safe navigable vessel clearance (Thies 2011). These two technologies combined provide a novel method of monitoring breakwaters (the 3D method). Detailed profiles and 3D models of the entire above water structure can be evaluated by high definition land based scanning and the underwater surfaces by the multi-beam echo sounding equipment. By using both techniques, a detailed geo-referenced data file is created of the structure by means of computer-aided design (CAD) software. The data are then processed to extract quantitative information, as proposed by (Phelp and Tulsi 2006).

The photographic method is presently the norm internationally for monitoring concrete armour damage. This is limited to the above water part of the breakwater only. Therefore an estimate of damage below the water is required. Using current LIDAR and multi-beam echo sounding methods underwater damage can now be determined.

## OBJECTIVE

The objective of this study is to test the 3D method by evaluating the accuracy of using the LIDAR and multi-beam echo sounder data to quantify damage to dolos breakwaters above and below the water surface, including the intertidal zone. Thus, this comparison is aimed towards the development of the 3D method. The study comprised two main components:

1. Physical model application: To compare the results (including progressive damage) from the 3D scanning method with the photographic method. Note that in a physical model (controlled environment), the water can be drained and both LIDAR scanning and taking of photographs can be done accurately.
2. Prototype application: To compare the damage calculated using the 3D method with the damage found by the photographic method, thus confirming the reliability of the 3D method.

---

<sup>1</sup> Built Environment, Council for Scientific and Industrial Research, P.O. Box 320, Stellenbosch, 7599, South Africa

<sup>2</sup> Department of Civil Engineering, Stellenbosch University, Private Bag X1, Matieland, 7602, South Africa

<sup>3</sup> Transnet National Ports Authority, Transnet, P.O. Box 4245, Cape Town, 8000, South Africa

<sup>4</sup> Geo-solutions, Horts Solutions, 44 Hiddingh Road, Bergvliet, Cape Town, 7945, South Africa

<sup>5</sup> Engineering Survey Department, CIVOC Engineering Services, P.O. Box 31600, Tokai, 7974, South Africa

### EXPERIMENTAL VERIFICATION

Breakwater design is usually based on the Hudson and van der Meer stability equations (USACE 2006). Damage assessment methods discussed are based on technologies of the past and require an update, using new technologies to better assess engineering structures in the attempt to provide more detail to interpret structure deterioration.

### ACCURACY TEST

The ability of the 3D scanner to capture minor, moderate and large movement on a dolos protected slope is investigated. To achieve this, damage is created manually by individually moving dolos units. The experiment was set-up in the CSIR Coastal and Hydraulics Laboratory, Stellenbosch. The dolos units scanned represent 30 tonne dolos with a station width of 27 m prototype scaled at 1:75. Two stations are monitored of width  $11 D_n$  each, namely station 1 and station 2.  $D_n$  in this case refers to the equivalent cube length of the armour unit. Station 1 was manipulated by creating damage by hand and station 2 was the control where no damage occurs.  $D_n$  of the model dolos represents 3.28 cm, and each station represents  $11 D_n = 36.16$  cm (model). Station 1 has a total of 190 dolos units and station 2 has 178 dolos units.

A fixed digital camera (Cannon DV-MV830i) was set-up on a tripod and focused perpendicular towards the slope. The camera was remotely controlled to limit any unnecessary movement or editing of the captured image to compare with other test images. This is followed by the 3D laser scanner which was also set-up perpendicularly to the slope with the same view as the fixed camera, as shown in Figure 1. The scanner was remotely controlled using a laptop computer.

The Riegl VZ-400 3D laser scanner was used for the experiment. The 3D laser scanner emits a laser pulse which is deflected by a polygonal mirror to its surroundings. The laser beam may hit one or many targets over the range of 600 m causing several echo pluses. The instrument's receiver records these reflected optical echo signals. The receiver converts the optical returns into electronic signals which are digitized for waveform processing. The waveform analysis calculates the optical echo signals by multiplying it with the known speed of light (299 792 458 m/s) leading to a point at a distance away from the scanner. The manufacturers specification indicates the scan data acquisition produces 5 mm accuracy with 3 mm precision and repeatability within a range of 600 m, (RIEGL 2012).

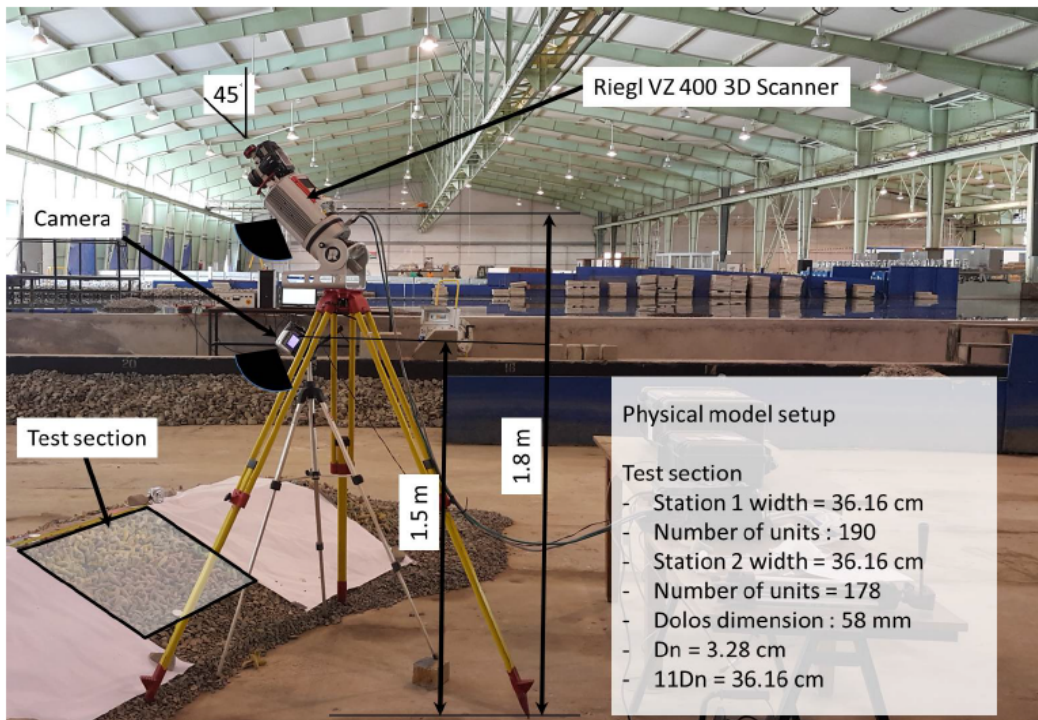


Figure 1: Laser scanner and fixed camera positioned over test section.

The digital image captured by the fixed camera is presented in Figure 2 (Left). It is used as a reference and analysed visually by blinking two images and tracking displacements. The 3D laser scanner is placed above the fixed camera to capture the same slope. The data captured from the laser scanner is meshed using 3DReshaper software to view and mesh the point data and project colour onto the surface (Figure 2 (Right)). The laser scan image is created from a data set of  $x,y,z$  points and colour returns captured by the scanner which are meshed to provide a quantifiable image in 3D. Both images are of the same slope using different technologies. The image taken by the camera is clear whereas the scanned image is dark yet picks up the entire slope of dolos units.



**Figure 2: Camera image of dolos slope (Left) , 3D laser scanner image of dolos slope (Right).**

The cross-section view shown in Figure 3 (Left) illustrate the profile track line spaced  $1 D_n$  apart. Due to the random placement of dolos and its complex shape cross-sections can be miss-interpreted as being irregular especially at a spacing of  $1 D_n$  apart. However with a 3D surface meshed overlay, the profiles are more easily recognised and can be interpreted as shown in Figure 3 (Right). The same profile view is presented in Figure 3 (Left) without the 3D image making it difficult to visualise the surface and less representative. The maximum deviation recorded on the slope between the ten repeated profiles was 6 mm. This was recorded near the edge of the profile. It should be noted that care should be taken when creating a mesh and it is advised to scan an area equal to 1.5 times the area of interest thereafter the focus area is cut out to improve the meshing of the data points along the boundary.

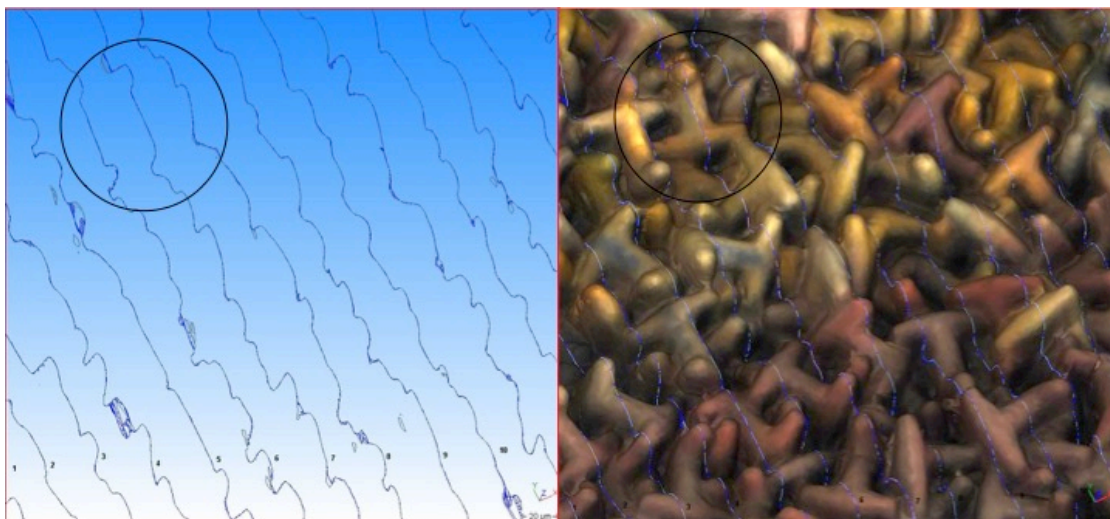


**Figure 3: Visual comparison between cross-sections (Left) and 3D mesh of dolos slope (Right).**

The cross-sections are used for volume calculations by interpolating between the parts between cross-sections. One surface is used as a reference and the others compared over or under the reference surface.

Therefore, the closer the spacing between profiles the better the accuracy. However, this may be difficult to achieve, as it will require excessive computing time. The spacing between profiles was therefore evaluated at  $1 D_n$ ,  $0.5 D_n$ ,  $0.25 D_n$ ,  $0.125 D_n$ ,  $0.0625 D_n$ , and  $0.03125 D_n$  to determine the most suitable in terms of processing time and accuracy. The finding of this investigation indicates there can be up to 19% improvement in calculating the volume difference by reducing the spacing to  $0.25 D_n$  between profiles. The results for volume calculations become similar at  $0.25 D_n$ , and  $0.125 D_n$ . The computations become impractical and time consuming when processing profiles are less than  $0.0625 D_n$  apart. It should be noted that due to the limitations in computing equipment the smaller  $D_n$  spacing was not possible. The selection of the spacing refines the 3D Reshaper software by forcing the volume calculation to be done at  $0.25 D_n$  by  $0.25 D_n$  intervals over the two meshes to calculate the accretion (overbreak) erosion (underbreak).

The profiles captured are easily produced for small scale physical model tests and spacing can be predetermined. Spacing of  $1 D_n$  apart provides a suitable average profile of the surface, however spacing of  $0.5 D_n$ ,  $0.25 D_n$  and  $0.0125 D_n$  were compared and shown in Table 1 by calculating the volume eroded between scan Test 1 and scan Test 3. The volume computed for the cross-sections taken at  $1 D_n$  apart deviated by 19%. This was the most extreme for this case. The most similar results were between  $0.5 D_n$ ,  $0.25 D_n$  and  $0.125 D_n$  with a deviation of 10%, and 9% respectively with reference to  $0.125 D_n$ . The processing time was however the fastest for  $1 D_n$  spaced cross-sections to determine the eroded volume. An attempt was made at reducing the gap between the cross-section to  $0.0625 D_n$  and  $0.03125 D_n$  however, processing times were in excess of 80 mins and computing power was limited.

**Table 1. Comparison of cross-sectional spacing and volume calculation.**

Spacing	Spacing	Profiles	Volume Eroded	Absolute Average Percentage Deviation	Processing time
$D_n$	mm	Unit	$m^3$	%	minutes
$1D_n$	32.8	11	8.99	19	15 min
$0.5 D_n$	16.4	22	12.131	10	20 min
$0.25 D_n$	8.2	44	12.059	9	35 min
$0.125 D_n$	4.1	88	11.024	0	55 min
$0.0625 D_n$	2.05	176	-	-	> 80 min, impractical to process
$0.03125 D_n$	1.025	352	-	-	> 80 min, impractical to process

#### DISPLACEMENT, ROTATION AND SETTLEMENT QUANTIFICATION

The experimental verification of the 3D method included tests ranging from minor movement to major displacement. The displacements were carried out by hand to control small movements, rotations, settlement and complete exposure down to the underlayer. The test data were recorded using the fixed camera and the 3D Laser scanner. The camera and 3D Laser scanner provide visuals therefore both are processed using the Armour Track software. Damage classification is carried out by visually counting displacements. To date, methods have been developed to quantify damage to rock armoured breakwaters using the average eroded area approach. Presently there is no information on classifying dolos armour unit damage using eroded volumes therefore a new method is described.

The analysis using this method quantified the displacement in terms of 0 to  $0.5 D_n$  displacement for minor settlement and movement,  $0.5$  to  $1 D_n$  displacements for intermediate movement and large displacements in terms of  $1 D_n$  to  $2 D_n$  and greater than  $2 D_n$ . The 24 Tests with reference to damage levels are listed in Table 2.

Table 2. Damage level criteria and test description for dolos displacement tests.			
	Initial	Intermediate	Failure
Damage Level Criteria	0-2%	3-14%	≥ 15%
Test Description	Test 1 to 6	Test 7 to Test 19	Test 20 to Test 24

To classify damage using the 3D eroded volume method some assumptions and recommendations were made with reference to the width of the test section and volume of the primary armour layer in this section to be able to compare visual quantification of damage to CAD volumetric quantification.

By adapting the relative eroded area method described by (Broderick 1982), the 3D eroded volume method is defined to analyse the design station. The average eroded area of each cross-section taken every  $D_n$  apart is used to determine the eroded area, see Eq. 1.

$$S = \frac{A_e}{D_n^2} \quad (1)$$

Where  $A_e$  refers to the average cross-sectional eroded area and  $D_n$  the nominal armour unit diameter. The 3D eroded volume method (Eq. 2) uses the station width i.e, one station can be the sum of  $11D_n = 36.16$  cm representing 27 m in the case of the test station Figure 1. Depending on the size of unit the stations will vary. It is recommended using 11  $D_n$  width as a station for ease of processing the data. This makes it possible to compare the photographic station damage with the multi-beam and laser scanning. The eroded volume is calculated using the 3D Reshaper CAD software to compute the eroded volume difference between the two profiles. This is computed at intervals of  $0.25 D_n$  across the width of the station. By including the station width, the equation is:

$$S_{3D}D\% = \frac{V_{station\ erosion}}{V_{station\ design}} \times 100 \quad (2)$$

Where  $V_{station\ erosion}$  refers to only the sum of the eroded volume of the station armour layer and  $V_{station\ design}$  the volume of the station armour layer including voids. The equation does not account for any accretion above the design surface. Therefore  $S_{3D}$  can be expressed as a percentage of the slope that is damaged and  $V_{station\ erosion}$  is computed from the comparison of the two scanned datasets to extract the volume eroded. The  $V_{station\ design}$  is the as-built volume created by a 3D shape of the slope. It is assumed for the investigation that  $S_{3D}D\%$  can be related directly to the damage level  $D\%$  for two-layer armour given in Table 2.

#### EROSION QUANTIFICATION COMPARISON USING VISUAL ANALYSIS AND 3D LASER SCANNING TECHNIQUE

The 3D laser scanning technique using eroded volumes to measure damage to dolos breakwaters was compared with the traditional visual analysis method. The test programme was carried out in stages:

1. Test 1 to Test 6: Minor movement less than  $0.5 D_n$ .
2. Test 7 to Test 16: Rotations of an individual unit until displacement out of the slope.
3. Test 17 to Test 19: Settlement tests.
4. Test 20 to Test 24: Major changes to the slope with units displaced to expose the underlayer.

The results of the displacement, rotation and settlement tests using the photographic method are presented below in Table 3. The 3D scanned eroded volume method is also shown in Table 4.



Test Description	Displacement				DT	Nd(%)	Nod(%)	D(%)
	0-0.5Dn	0.5Dn-1Dn	1Dn-2Dn	≥2Dn				
initial damage (1)T1.1	0				0.0	0.0	0.0	0.0
initial damage (2)T1.2	0				0.0	0.0	0.0	0.0
initial damage (3)T1.3	1				0.5	0.0	0.0	0.0
initial damage (4)T1.4	0				0.0	0.0	0.0	0.0
initial damage (5)T1.5	1				0.5	0.0	0.0	0.0
initial damage (6)T1.6	1				0.5	0.0	0.0	0.0
intermediate (7)T2.1		1			1.0	0.0	0.0	0.0
intermediate (8)T2.2		1			1.0	0.0	0.0	0.0
intermediate (9)T2.3		1			1.0	0.0	0.0	0.0
intermediate (10)T2.4			1		1.0	0.5	0.8	2.8
intermediate (11)T2.5			1		1.0	0.5	0.8	2.8
intermediate (12)T2.6			1		1.0	0.5	0.8	2.8
intermediate (13)T2.7			1		1.0	0.5	0.8	2.8
intermediate (14)T2.8				1	1.0	0.5	0.8	2.8
intermediate (15)T2.9				1	1.0	0.5	0.8	2.8
intermediate (16)T2.10				1	1.0	0.5	0.8	2.8
intermediate * (17)T3.1	25			1	13.5	0.5	0.8	2.8
Intermediate ** (18)T3.2	34			1	18.0	0.5	0.8	2.8
intermediate *** (19)T3.3	37			1	19.5	0.5	0.8	2.8
Failure (20)T4.1	37			7	25.5	3.7	5.9	19.7
Failure (21)T4.2	37			7	25.5	3.7	5.9	19.7
Failure (22)T4.3	39			7	26.5	3.7	5.9	19.7
Failure (23)T4.4	39			11	30.5	5.8	9.3	30.9
Failure (24)T4.5	40			11	31.0	5.8	9.3	30.9

\* Settlement minor

\*\* Settlement moderate

\*\*\* Settlement major

Test Description	Displacement		Volume (cm <sup>3</sup> )	S <sub>3D</sub> D(%)
	Overbreak (accretion)(cm <sup>3</sup> )	Underbreak (erosion) (cm <sup>3</sup> )		
initial damage (1)T1.1	7.113	2.462		0.0
initial damage (2)T1.2	2.435	3.254		0.0
initial damage (3)T1.3	4.054	1.162		0.0
initial damage (4)T1.4	3.83	3.51		0.0
initial damage (5)T1.5	8.816	5.492	2.46E-02	1.6
initial damage (6)T1.6	1.49	5.006	3.25E-02	2.1
intermediate (7)T2.1	1.905	7.756	1.16E-02	0.7
intermediate (8)T2.2	4.659	2.808	3.51E-02	2.2
intermediate (9)T2.3	4.855	4.716	5.49E-02	3.5
intermediate (10)T2.4	2.339	4.643	5.01E-02	3.2
intermediate (11)T2.5	17.93	9.725	7.76E-02	4.9
intermediate (12)T2.6	1.931	3.081	2.81E-02	1.8
intermediate (13)T2.7	4.529	7.037	4.72E-02	3.0
intermediate (14)T2.8	9.988	9.722	4.64E-02	2.9
intermediate (15)T2.9	9.069	15.459	9.73E-02	6.1
intermediate (16)T2.10	12.547	23.164	3.08E-02	1.9
intermediate * (17)T3.1	6.795	28.748	7.04E-02	4.4
Intermediate ** (18)T3.2	16.611	38.358	9.72E-02	6.1
intermediate *** (19)T3.3	14.211	33.945	1.55E-01	9.8
Failure (20)T4.1	5.026	35.332	2.32E-01	14.6
Failure (21)T4.2	7.113	2.462	2.87E-01	18.1
Failure (22)T4.3	2.435	3.254	3.84E-01	24.2
Failure (23)T4.4	4.054	1.162	3.39E-01	21.4
Failure (24)T4.5	3.83	3.51	3.53E-01	22.3

\* Settlement minor

\*\* Settlement moderate

\*\*\* Settlement major

The results of the 24 tests are presented in Figure 4. The model displacement is presented as cumulative damage percentage in relation to the changes based on the first image and/or the data from the scanner. The percentage damage is calculated in two ways for the two data sets. The digital camera analysis which uses the Armour Track software and the second the 3D method which uses the 3D Reshaper software. The digital camera photograph analysis is calculated by counting the number of

displacements explained by Holtzhausen et al 2000, van der meer (1988) and Burcharth and Lui (1992). The second method uses Eq. 2 to calculate the cumulative damage percentage by the 3D scanned eroded volume method.

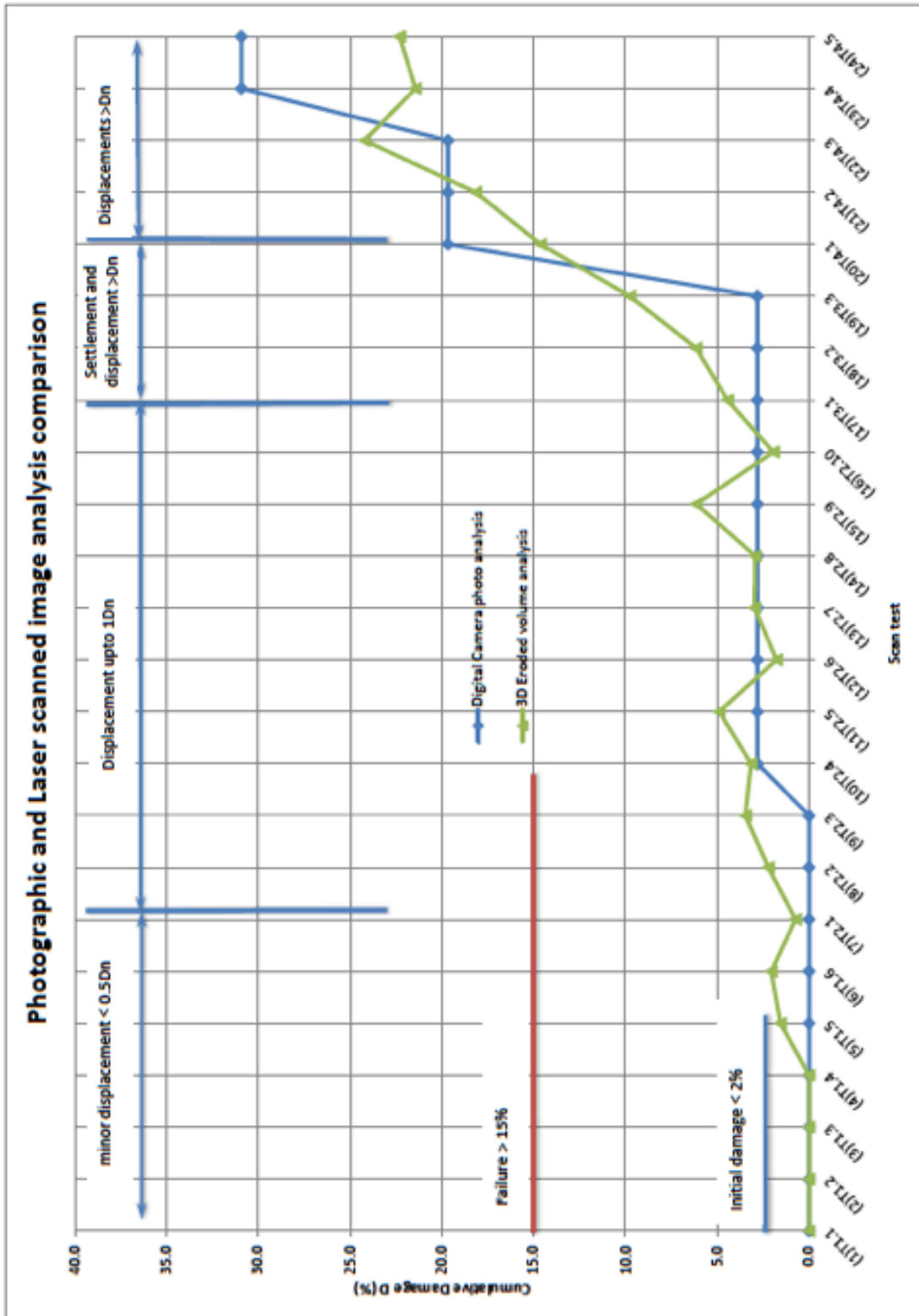


Figure 4: Comparison between 3D eroded volume (Green line) and visual (blue line) analysis.

### PHYSICAL MODEL SUMMARY

The outcome of the investigations indicated the accuracy of the measurements depended on the ability to process and create a mesh of the scanned data, therefore previously photographic and manual methods proved to provide more accurate results in the past. Nowadays, mesh generation has improved and individual armour units can be recognized in mesh form similar to photographs. In this experimental verification the 3D scanned data were dense with limited shadows and coverage problems were reduced by the angle of the scanner and height above the dolos slope which made data capture suitable for analysis. This is also the case for the photographs taken in this experiment using the traditional methods. The repeatability tests provided information on the reliability of repeated scans in this controlled environment which gives confidence when comparing identical scans. The repeatability tests were carried out by comparing 10 consecutive scans with the first scan. The standard deviation was  $0.001 \text{ cm}^3$  when comparing the ten scans. A cross-sectional analysis was also carried out as part of the repeatability tests in tracking the variation in extracting cross-sections. The difference between scans was negligible with the maximum being 6 mm found at the edges of the cross-section.

The process of extracting the eroded volumes requires a minimum of two cross-sections on either end of the station. This can be improved by creating more cross-sections. The ability to track the intricate shape of the dolos unit was tested and cross-sections were taken at intervals of  $1D_n$ ,  $0.5 D_n$ ,  $0.25 D_n$ ,  $0.125 D_n$ ,  $0.0625 D_n$  and  $0.03125 D_n$ . Cross-sections between  $1 D_n$  to  $0.125 D_n$  were possible with the optimal cross-section being limited to  $0.25 D_n$  due to limitations in computing power. This is important for the volume calculations as the closer the cross-section interval the more accurate the volume calculation. The most similar results were found between  $0.5 D_n$ , and  $0.25 D_n$ . The method can be made more accurate in future depending on the processing speed and memory of the computer, therefore smaller spacing can be used. However, for this application  $0.25 D_n$  was used in the computations.

Twenty four (24) tests were carried out to quantify the expected damage percentage that can be associated with displacement, rotation and settlement using the eroded volume method. This was compared with the visual method. Damage percentages for both methods are plotted in Figure 4. The damage classification used was Van der Meer (1988) for the damage parameter  $D\%$ . The method indicates there are variations factor of two times between the two methods for some individual results however the results have a similar trend when comparing all twenty four tests.

Both methods are able to track differences in the slope if there is settlement, minor displacements and rotations to calculate a damage percentage in relation to the first scan or first image. Improving the mesh triangulation grid spacing and edge detection to improve intricate surfaces for eroded volume calculations can further refine the 3D eroded volume method.

### FIELD APPLICATION

The Port of Cape Town is located in Table Bay, Western Cape, South Africa. The breakwater trunk spans 500 m south to north and is protected by 25 tonne dolosse. The spur section as shown in Figure 5 was scanned to correlated damage percentage using the 3D method.



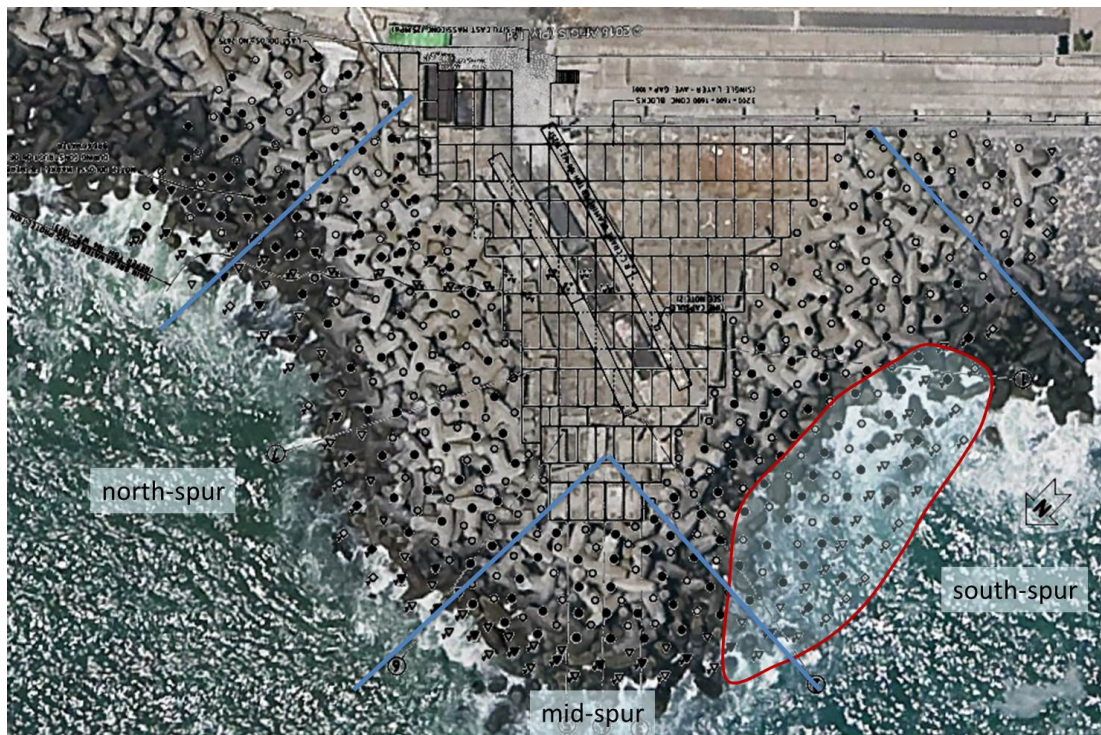


Figure 5: Plan view of spur breakwater at the Port of Cape town, South Africa.

This section presents the set-up of the data collection using the laser scanner and multi-beam sonar equipment. Three-dimensional (3D) high definition data set is analysed using the standard damage assessment techniques of area calculation compared with an alternative volumetric method. A quantitative assessment is made using the eroded area against 3D isometric sections of the eroded volume. The hydrographic survey (multi-beam and LIDAR Laser scan) was conducted from a 6 m long ski-boat which was very manoeuvrable in the surf-zone and close to the breakwater. The survey was done during calm sea conditions. The survey was conducted at low and high tide on the same day. The operating water depth was between 5 m and 20 m. During low tide, the laser scanning was carried out and during high tide the multi-beam soundings were done. The purpose of this is to ensure there is a seamless transition between the above water and below water data collection. This is a critical step in the data capture and should be ensured or the survey should be repeated on another day if there is no overlap. Ideally both sets of equipment should be capturing data simultaneously throughout the day however this would require a duplication of the inertial moment unit.

The data from the multi-beam echo sounder provided the bathymetric information of the structure below the water surface. The laser scanner provided the topographic levels of the breakwater above the water line. Figure 6 below shows a schematic drawing showing how the multi-beam and laser scanner covered the survey area from the survey boat. A list of equipment used to conduct the survey is provided below.

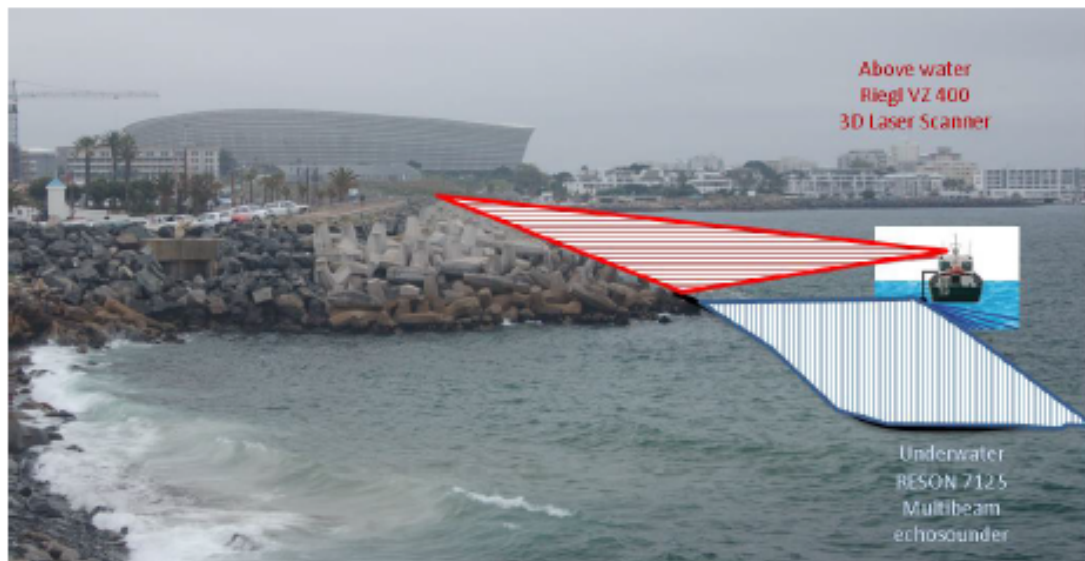


Figure 6: Multi-beam and mobile laser scanner capture area

The equipment used for the survey include:

1. Reson Seabat 7125 multi-beam echo sounder - for the capturing of 3D data.
2. Applanix POS MV 320 position, heading and motion sensor for attitude and heading correction.
3. Reson SVP-70 sound velocity probe for sound velocity correction.
4. Leica GX1230 GNSS RTK DGPS positioning system for water to land positioning.
5. Reigl VZ400 – HD Laser scanner

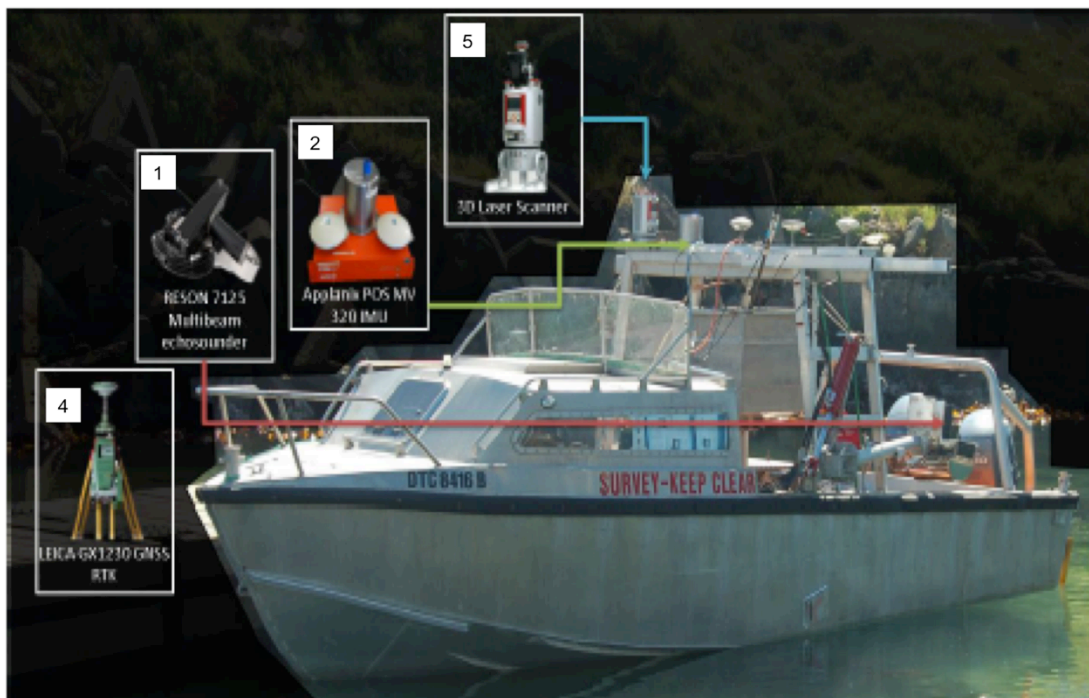


Figure 7: Multi-beam and mobile laser scanner on boat set-up for the breakwater survey



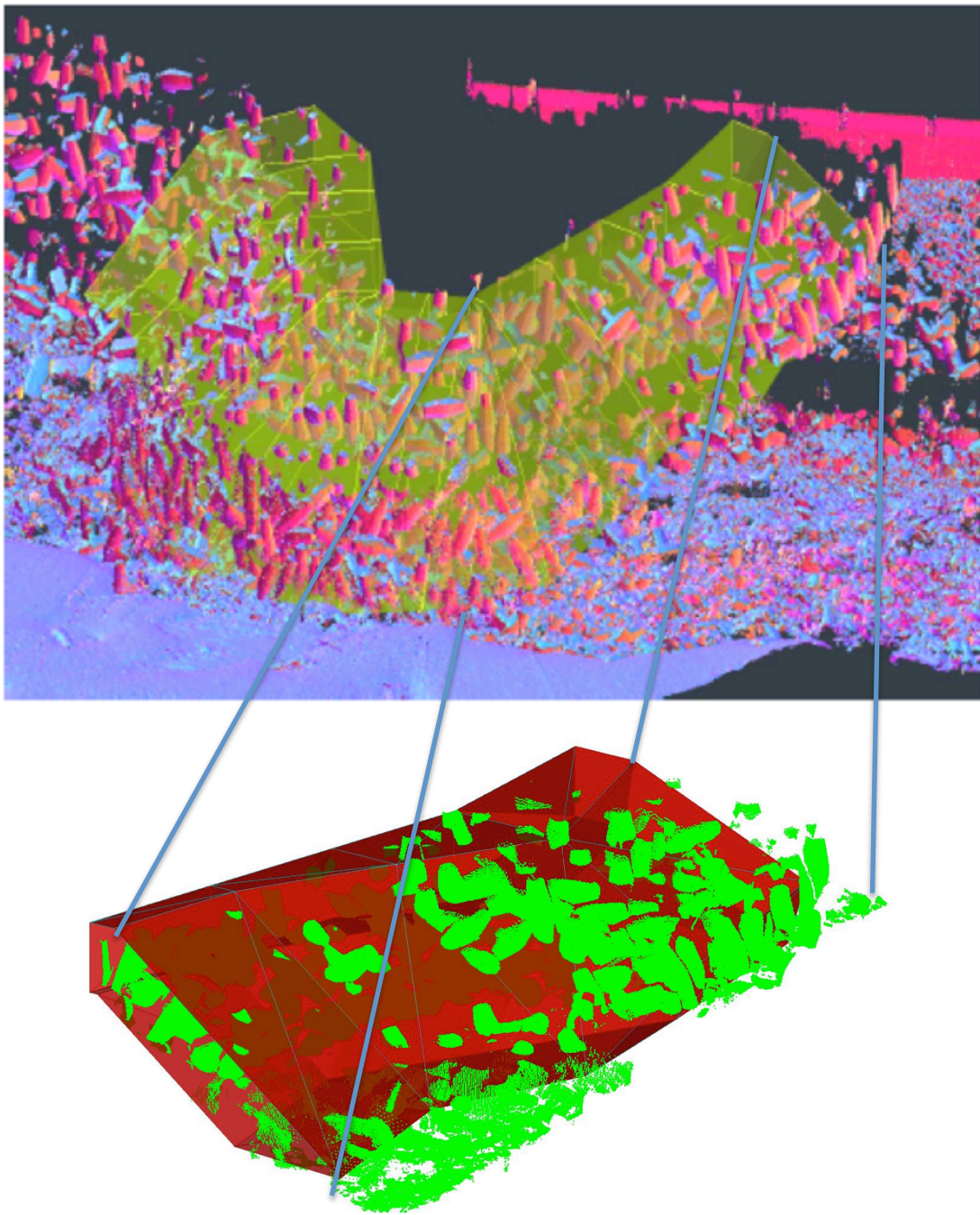


Figure 8: Multi-beam and laser scanner south west aerial view and cross-section through the mesh

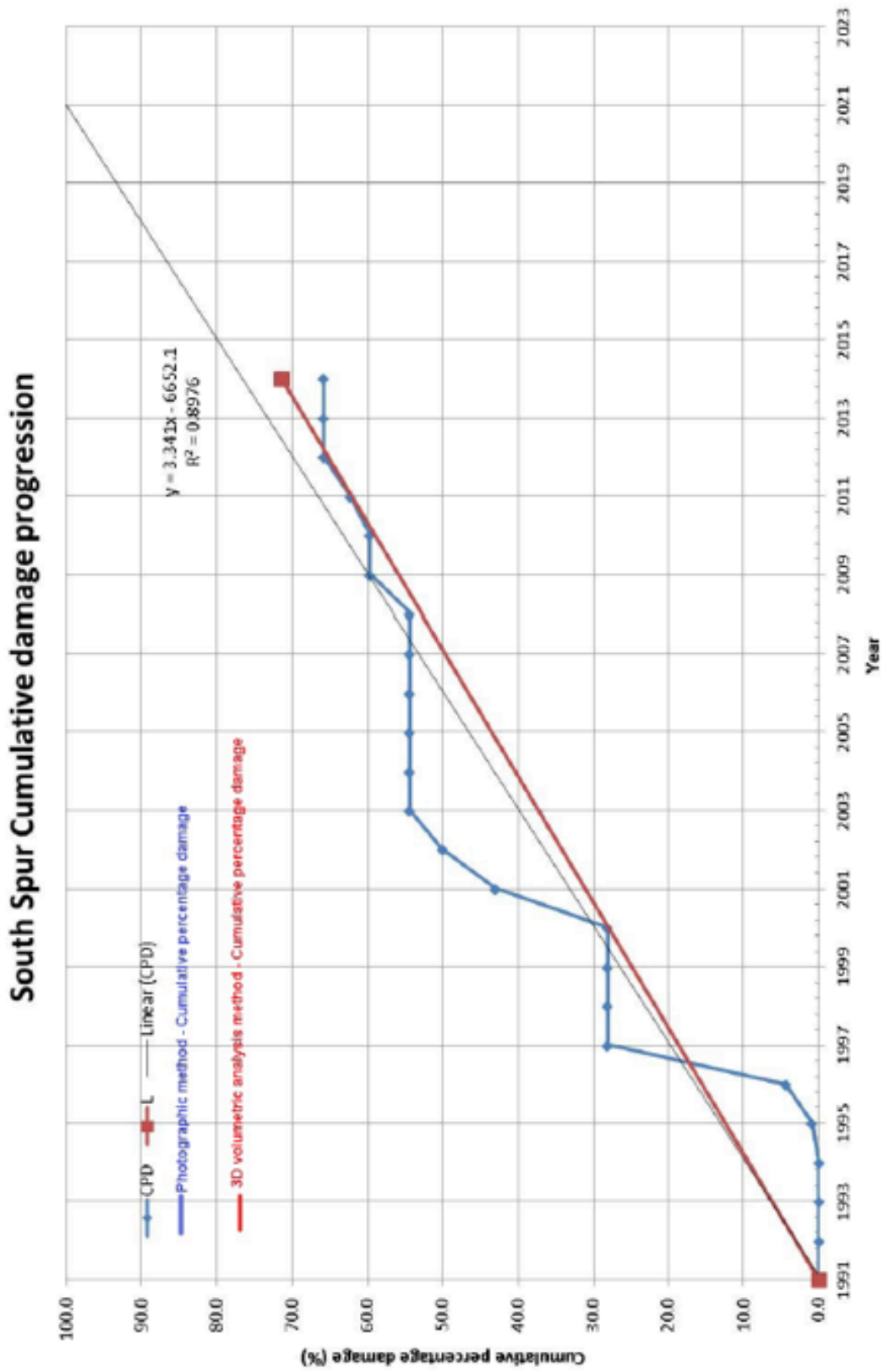


Figure 9: Cumulative percentage damage from photographic and 3D method analysis

The result of the photographic analysis indicates the present damage to the breakwater is 65.8%. The three dimensional eroded volume analysis indicates the damage to be 71.4%. The difference between the two calculation methods is 5.6%. The figure shows the cumulative percentage damage over time. This can be updated in future to track the performance of the two methods.

### CONCLUSIONS AND RECOMMENDATIONS

The experimental verification of the 3D method considered tests with minor movement to major displacement. The displacements were carried out by hand to control small movements, rotations, settlement and complete exposure down to the underlayer. The tracking of damage progression from minor movement, to rotational displacements and major movement produced similar damage percentage trends to the photographic visual method. The findings of the cumulative percentage damage indicates that the difference between the 2D visual method damage level by  $D(\%)$  and 3D scanned eroded volume method  $S_{3D}D(\%)$  follow a similar damage progression trend however, some individual results differ for example Test 19 which can differ in magnitude of three times the damage level.

The physical model experimental application compared the results including progressive damage calculated by the 3D method with the photographic method of a 1:1.5 dolos slope in a controlled environment. The test program was carried out in stages from minor movement less than  $0.5 D_n$  (Test 1 to Test 6), rotations of an individual unit until displacement out of the slope (Test 7 to Test 16) followed by settlement tests (Test 17 to Test 19) and finally major changes to the slope with units displaced to expose the underlayer (Test 20 to Test 24). The findings of the cumulative percentage damage indicates that the difference between the 2D visual method damage level by  $D(\%)$  and 3D scanned eroded volume method  $S_{3D}D(\%)$  follow a similar damage progression trend however, some individual results differ for example Test 19 which can differ in magnitude of three times the damage level.

The prototype application calculated using the 3D method compared with the damage found by the 2D photographic method, compares well, thus confirming the suitability of the 3D method in prototype. This also confirms that the settlement and displacement voids are being recorded of the entire breakwater slope from toe to crest. This also indicates that 3D analysis method results in prototype are conservative. The trend line of the photographic method and that of the 3D method correlate well. This method has shown that the combination of laser scan and multi-beam measurements from a mobile platform can replace the aerial photographic procedures especially if data is required between the intertidal zone, down to the toe. It can be accepted that the 3D scanned eroded volume method (3D method) realistically reflects the quantification of damage progression.

### REFERENCES

- Broderick, L., 1982. 'Rip-rap stability scale effects', pp. 82–3.
- Burcharth, H., D'Angremond, K., van der Meer, J. and Liu, Z., 2000. 'Empirical formula for breakage of dolosse and tetrapods', *Coastal Engineering* 40(3), 183–206.
- Holtzhausen, A., Retief, G. d. F. and Zwamborn, J. A., 2000. Physical Modelling of Dolos Breakwaters: The Coega Results and Historical Perspective, in '*Coastal Engineering 2000*', pp. 1536–1549.
- Phelp, D. and Tulsi, K., 2006. Digital image technology as a measurement tool in physical models, in '*International Conference on the Application of Physical Modelling in Coastal and Port Engineering and Science*', pp. 21–31.
- Phelp, D. and Zwamborn, J., 2000. 'Correlation between model and prototype damage of dolos breakwater armouring', *Coastal Engineering 2000* pp. 1–13.  
 URL: [http://ascelibrary.org/doi/abs/10.1061/40549\(276\)120](http://ascelibrary.org/doi/abs/10.1061/40549(276)120)
- RIEGL, 2012. '3D Terrestrial Laser Scanner, RIEGL VZ-400 / RIEGL VZ-1000'.
- Thies, T., 2011. A Vessel-Based mobile mapping system from sensor integration to multipurpose products, PhD thesis, University Hamburg, Germany.  
 URL: [http://www.riegl.com/uploads/tx\\_pxpriegldownloads/Thies\\_Thomas\\_2011 -  
 - A Vessel-Based Mobile Mapping System Master Thesis HafenCity University - Hamburg  
 Germany part1.pdf](http://www.riegl.com/uploads/tx_pxpriegldownloads/Thies_Thomas_2011_-_A_Vessel-Based_Mobile_Mapping_System_Master_Thesis_HafenCity_University_-_Hamburg_Germany_part1.pdf)
- Tulsi, K. and Phelp, D., 2009. Monitoring and maintenance of breakwaters which protect port entrances, in '*28th Annual Southern African Transport Conference*', number July, pp. 317–325.

**URL:** <http://hdl.handle.net/2263/12016>

USACE, 2006. [CEM] Engineer Manual, in W. CHL-ERDC, ed., *Coastal engineering manual*, Vicksburg,MS, pp.1110–2–1100.

Van der Meer, J. W., 1988. Rock slopes and gravel beaches under wave attack, PhD thesis, Delft Hydraulics Laboratory, Emmeloord, The Netherlands.